



# ACOUSTIC EMISSION BASED DEFECTS MONITORING OF THREE-DIMENSIONAL BRAIDED COMPOSITES USING WAVELET NETWORK

Su Hua<sup>\*,1</sup>, Zhang Tianyuan<sup>1</sup> and Zhang Ning<sup>1</sup>

<sup>\*,1</sup>Tianjin Polytechnic University, Binshui Road 399,  
Xiqing District, Tianjin, 300387, P.R. China

Email: hua\_207@126.com

---

*Submitted: Nov. 7, 2015*

*Accepted: Jan. 22, 2016*

*Published: June. 1, 2016*

---

*Abstract- In order to effectively differentiate all kinds of defects inside the composites, this paper carries out testing on the internal defects of three-dimensional (3d) braided composites by use of acoustic emission nondestructive detecting technology. It puts forward the processing method for acoustic emission signals for the internal defects of three-dimensional braided composites based on wavelet neural network (WNN). This method does wavelet transformation on real-time collected acoustic emission signals, takes the characteristics of internal defect energy to be obtained as network input, selects the wavelet neural network (WNN) with “compact” type and realizes the recognition on the classification of micro cracks and pores of 3d braided composites.*

**Index terms:** Three-dimensional (3d) Braided Composites, Acoustic Emission Detection, Wavelet Neural Network (WNN), Defect Detection.

## I. INTRODUCTION

Three-dimensional braided composite is a new type of 3d braided prefabricated reinforced composite [1]. Compared with other composite materials in performance, it has excellent characteristics such as specific strength, high specific modulus and good impact resistance. Therefore it has been widely used in fields like construction, medical treatment and aerospace & aircraft manufacturing, etc. [2] However, due to the special manufacturing process of three-dimensional braided composites, defects such as porosity, crack and inclusion will be formed inside the material, which will accordingly affect the longitudinal & lateral tensile intensity, bending strength, modulus, compressive strength and fatigue limit of the three-dimensional braided composites.

Many scholars have done a great amount of research on the fatigue damage mechanism of composites. Wan Zhenkai and Wan Zhangang[3] described the ultrasonic method detecting the inner flaw of three-dimensional braided composite materials. After the wavelet packet transform of three-dimensional braided composite material ,a scan echo of ultrasonic, the material's inner defection signal is expressed as energy characteristics after it is extracted and decomposed. Input the feature values of the defections into BP neural Network which realizes classification and automated identification for micro-cracks and pores of three-dimensional braided composite materials. The experimental results proved that the method is feasible for detecting three-dimensional braided composite materials' inner flaws, but the method is not suitable for on-site monitoring. Wenfeng Hao et al.[4] investigated the fatigue behavior of 3D 4-directional braided composites based on the unit cell approach. Drach et al. [5] proposed an efficient procedure to process the textile simulation data and generate realistic finite element meshes of woven composites. Dong et al. [6]studied tensile strength of 3D braided composites in the microscopic view, where non-linear progressive damages under tensile loading steps were conducted in their article. In addition, there are a large number of studies using AE to analyze the damage process of carbon fiber and glass fiber composite [7-8] However, under the influence of factors such as material properties and test environment, AE wave is often shown as a complex, non-stationary, and random signal, containing a variety of noise. Therefore, finding an effective method of signal analysis is particularly important. Wavelet analysis uses a family of wavelet basis function to represent or approach signals and solves the conflicts of time-frequency resolution.

This paper utilizes wavelet neural network pattern recognition technology to do pattern recognition analysis on the acoustic emission signals of three-dimensional braided composites so as to find the internal defects of materials as soon as possible and provide certain basis for the confirmation of the early damage of three-dimensional braided composites. [9-10]

## II. 3D-4DIR BRAIDED COMPOSITES

The integrated structure of three-dimensional (3D) and four directional (4Dir) braided composites can improve the TOS of the CFPMCs by enhancing the ability of the fibers to bear the external load and resist delamination, despite the deterioration in the matrix resin and interface properties after thermo-oxidative aging (TOA) for long periods of time[5]. The basic braiding process involves four distinct motions of rroups of yarns termed rows and columns. For a given step, alternate rows are shifted a prescribed distance relative to each other. The next step involves the alternate shifting of the columns a prescribed distance. The third and fourth steps are simply the reverse shifting sequence of the first and second steps, respectively. A complete set of 4-directionals is called a machine cycle, which is shown in Figure 1. The 3D-4Dir braided architecture is illustrated in Figure 2. It is characterized by almost all the braider yarns being offset at different angles between the in-plane and through thickness directions, which can be seen clearly from the tracer yarn (colored yarns). An idealized model of the braid preform surface is shown in Figure 3, where  $h$  is the braiding pitch length,  $\alpha$  is the braiding angle[11]. The final specimens are illustrated in Figure 4

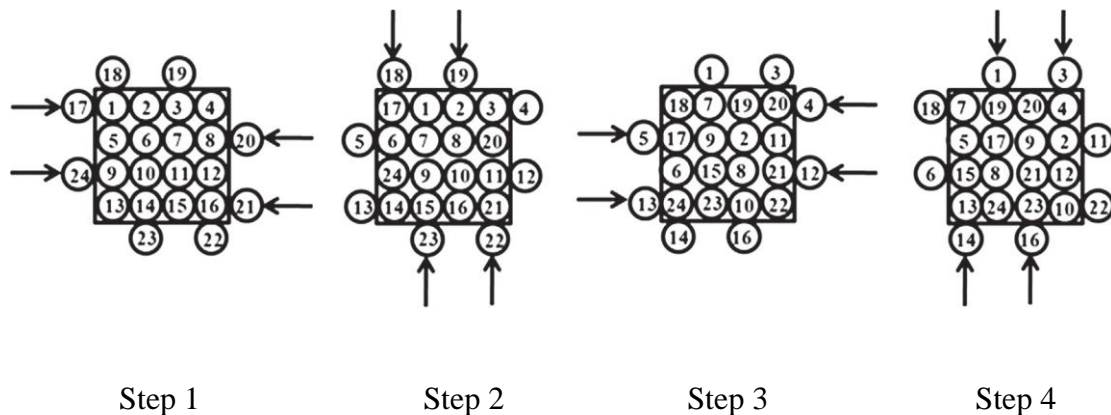


Figure 1. Braiding process of 3D 4-directional braided composites [12].

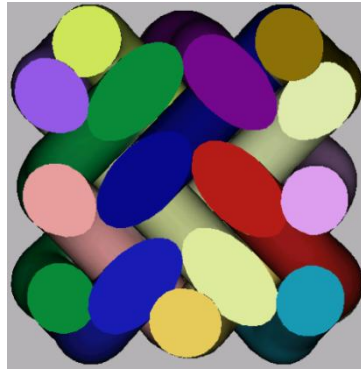


Figure 2. three-dimensional(3D) and four-directional(4Dir) braided architecture

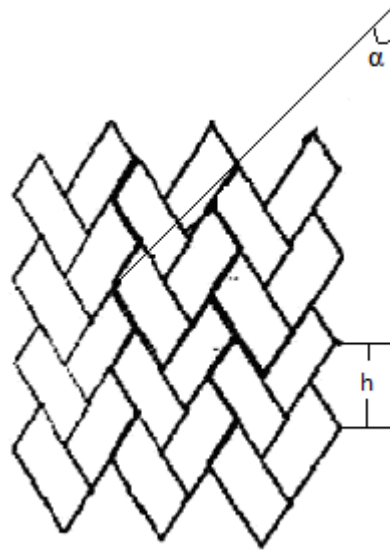


Figure 3. an idealized model of the 3D-4Dir braided preform surface



Figure 4. Drawing for Finished Product of 3-D Braided Composites.

### III. WAVELET NEURAL NETWORK (WNN)

The concept of Wavelet Neural Network (WNN) was firstly proposed by Qin Huazhang and other people in French information agency IRISA in the year 1992. It is the outcome of the development and integration of wavelet analysis theory and artificial neural network to a certain degree. Wavelet Transform (WT) does multi-scale analysis on signals through scale extension & compression & translation and is able to effectively extract the local information of signals; and the neural network has the characteristics such as self-learning, self-adaption and fault tolerance and it is a kind of universal function approximator. The primitives and the entire structure of wavelet neural network (WNN) are determined according to the theory of wavelet analysis and this can avoid the blindness of structural design in BP neural network and so on. At the same time, it has stronger ability to learn and higher precision. For the same learning tasks, wavelet neural network (WNN) owns simpler structure and faster convergence speed. Therefore wavelet neural network (WNN) has gained more and more application and promotion in fields like predictive control, signal processing, pattern recognition, fault detection & diagnosis. [12][14][15]

#### a. Structure of Wavelet Neural Network

Wavelet neural network can be divided into two types including “loose type” and “compact type” according to wavelet transform and combining ways of neural network. The former is the combination of form and the latter is an organic integration of both essentially.

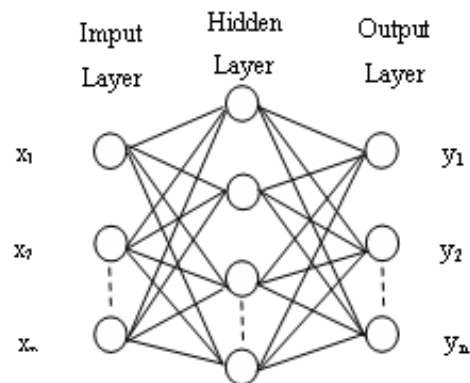


Figure 5. Chart for Three Layers of Network Structure

This paper selects widely-used wavelet neural network with “compact” type(as shown in Figure 5), which means that the wavelet element are replaced by neurons and the weights from input layer to hidden layer and the threshold in hidden layer are respectively replaced by the scaling and translation parameters of wavelet function. The network learning algorithm is as follows:

$$y_i(t) = f \sum_{j=0}^n w_{ij} \psi_{(a,b)} \left( \frac{\sum_{k=0}^m w_k x_i(t) - b_h}{a_h} \right) \quad (1)$$

The error function can be reached by gradient descent method:

$$E(i) = \frac{1}{2} f \sum_1^n (y_i(t) - y_i)^2 \quad (2)$$

$a_h$ : The contraction-expansion factor of the node h in hidden layer

$b_h$ : The translation factor of the node h in hidden layer

$w_k$ : The weight connecting the node k in input layer and the node j in hidden layer

$w_{i,j}$ : The weight connecting the node j in hidden layer and the node i in output layer

$y_i$ : Network target output

$$w_k(t+1) = w_k(t) - \eta \frac{\partial E}{\partial w_k} + \lambda \Delta w_k \quad (3)$$

When wavelet neural network is not consistent with the expected output, the output error E exists. And the output error E is the function of the weight  $w$ , scale parameter  $a_h$  and translation parameter  $b_h$ . If you need to reduce the errors constantly, you may need to adjust the network parameters. Thus you should make the adjustment quantity of network parameters be proportional to the negative gradient of errors. To further avoid the occurrence of oscillation in training process and improve the training speed of network, you can add a momentum in parameter formula. Thus in this way the following wavelet neural network (WNN) parameter correction formula is available:

$$w_{ij}(t+1) = w_{ij}(t) - \eta \frac{\partial E}{\partial w_{ij}} + \lambda \Delta w_{ij} \quad (4)$$

$$a_h(t+1) = a_h(t) - \eta \frac{\partial E}{\partial a_h} + \lambda \Delta a_h \quad (5)$$

$$b_h(t+1) = b_h(t) - \eta \frac{\partial E}{\partial b_h} + \lambda \Delta b_h \quad (6)$$

It can be seen from the above that the addition of momentum item can get some part of parameters from the previous parameter adjustment quantity and superpose them to the current parameter adjustment quantity. Here  $\lambda$  is the momentum factor. It reflects the accumulated adjustment experiences before and it can play a damping role in the adjustment at new moment. When there are sudden ups and downs in error curved surface, the oscillation trend can be reduced and the convergence speed can be accelerated. The flow of training is illustrated in figure 6.

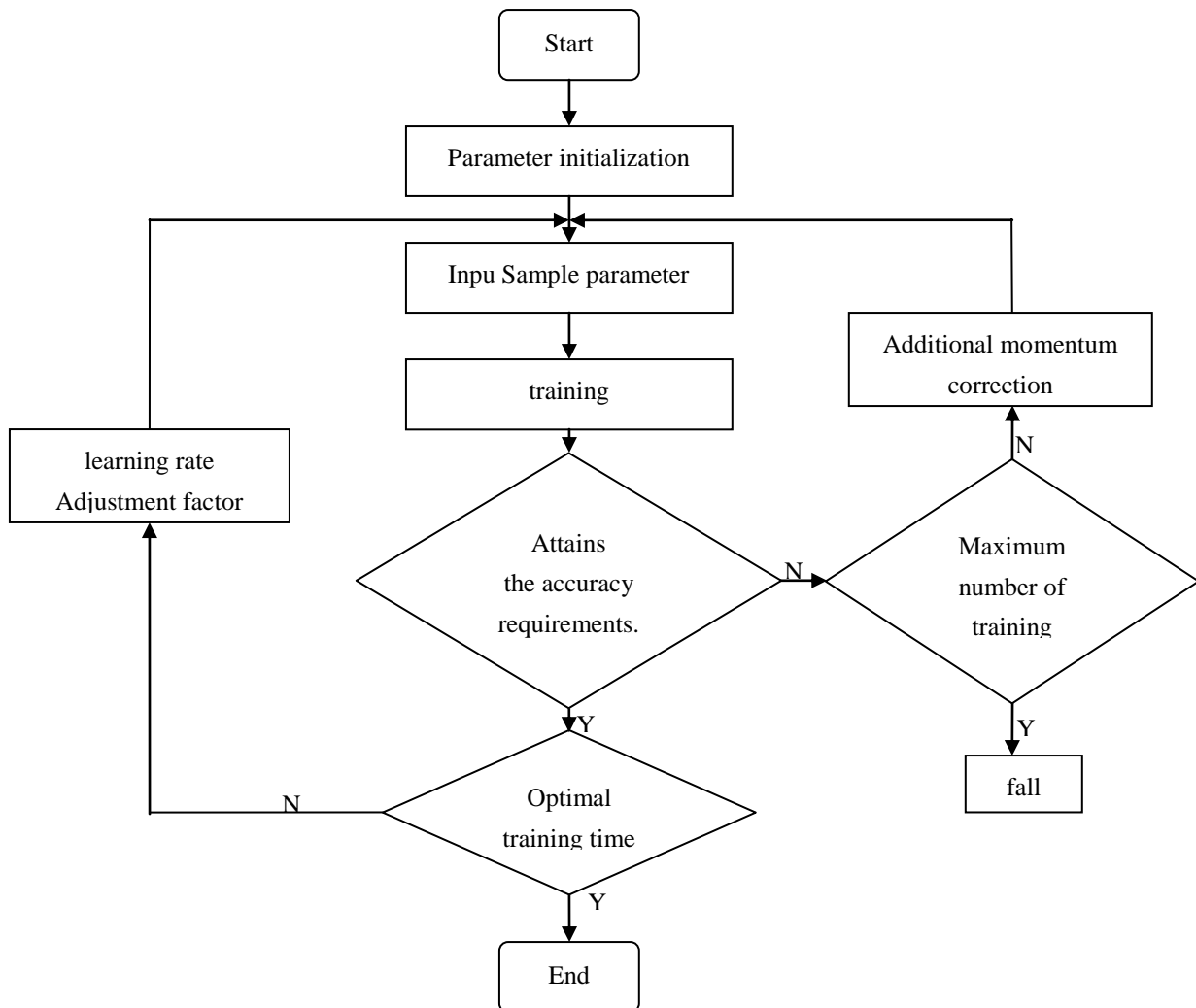


Figure 6. The Training Flew Chart

#### b. Confirmation on Number of Nodes in Hidden Layers

The number of nodes in hidden layers is also very important for the entire network performance. If the number is too tiny, the network can only get insufficient information from samples and it cannot fully reflect the inner law of samples. And this can further lead to the reduction of the generalization ability of network; and if the number is too much, the learning time of network can be increased, resulting in the reduction of convergence speed. At present, the selection of the number of nodes in hidden layers does not have an explicit analytic expression and it often needs to be determined by combining actual problems and carrying out several experiments. This paper combines the actuality and estimates the number of nodes according to the requirements of error precision and material characteristics. The design of number of nodes in hidden layers can be realized through formula (7).

$$n = 2n_{in} + 1 \quad (7)$$

In this formula,  $n$  represents the number of nodes in hidden layer of BP network; and  $n_{in}$  is the number of input nodes in hidden layer of BP network.

By calculation, the number of nodes in hidden layer of BP network in this system is 17.

In order to extract the eigenvalue of the wavelet packet decomposition of acoustic emission signals of internal defects in three-dimensional braided composites, the system extracts eight eigenvalues for each defect signal of 3d braided composites. So the number of input nodes of network is also set to eight. The system mainly identifies whether inside the composites exist the defect of pores or micro cracks. There are two outputs in the output layer of network. According to formula (7), it is calculated that when the number of nodes in hidden layer is 17, the network structure shall be determined as 8-17-2 type.

### IV. EXPERIMENTS RESULTS AND ANALYSIS

#### a. Experimental Specimens

The reinforced fiber of plate specimen in 3d braided composites adopts TORAYCCA@ T300 carbon fiber (12K). The prefabrication braided structure is four-step 1×1 3D & 5D woven structure and the substrate material is TDE86# epoxy resin. It uses resin transfer molding (RTM) technique for its curing and

molding and the thickness of specimens is  $(5 \pm 0.1)$  mm. There are totally 9 kinds of specimens for experiment.



Figure 7. SAEU2S Acoustic Emission System

#### b. Acoustic emission system

In this paper, it chose Soundwel Technology SAEU2S acoustic emission system (as shown in figure 7.) which can collect and display the waveform and parameters of the acoustic emission signal in real time. The SAEU2S is composed of a plurality of parallel detection channel acoustic emission system. Each channel of the system comprises a sensor, a preamplifier and a acquisition card for detecting acoustic emission signals. The basic structure of SAEU2S acoustic emission system is shown in figure 8

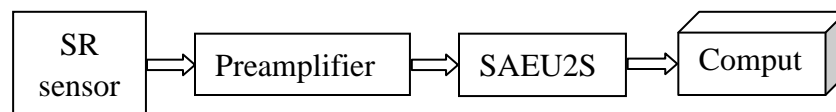


Figure 8. Basic Structure Cell of SAEU2S Acoustic Emission System

#### b.i Sensor

Since the frequency of the acoustic emission signal of the test piece is between 50K and 200K, the system selects a single ended resonant sensor. The model of sensor is SR150A .Its parameters are shown in Table1.

#### b.ii Preamplifier

The preamplifier is placed near the sensor to enlarge the signals and transmit them to a computer. The preamplifier main role is to: high-impedance sensors and low-impedance matching between transmission lines and to reduce the signal attenuation; through the amplification of weak input signal cable noise suppression to improve the signal to noise ratio; provide frequency filtering. Main amplifier and filter is an important component of the system.

Table1: the parameters of SR150A

Size (mm)	Weight (g)	Temperature	Frequency Range	Resonant Frequency	Peak Sensitivity
$\Phi 18.3 \times 14.5$	20	-20~80°C	50~400KHz	150KHz	> -65dB

The main amplifier provides the acoustic emission signal further amplification in order to follow-up measurement and calculation of parameters of signal processing units [11]. It has adjustable magnification, so that the gain of the entire system to achieve 60 ~ 100 dB. In the detection system is mainly used to add filters to exclude noise and limit the detection frequency range of systems to adapt to the noise in more complex testing environment. By the amplifier and filter treated by A/D converter for digital conversion, it is followed by a computer for further analysis.

The preamplifier of the syetem is PAI(as shown in Figure ). Its bandwidth range is 10KHz-2MHz,and the gain is  $40\text{dB} \pm 1\text{dB}$ . The peak noise is less than  $8\mu\text{V}$ . The dynamic range is greater than 74dB. The maximum output is greater than 20V and maximum input is greater than 200mV. The non - distortion output is greater than 13V. The principle structure of the experiment is shown in Figure 9. Figure 10 shows a kind of preamplifier.

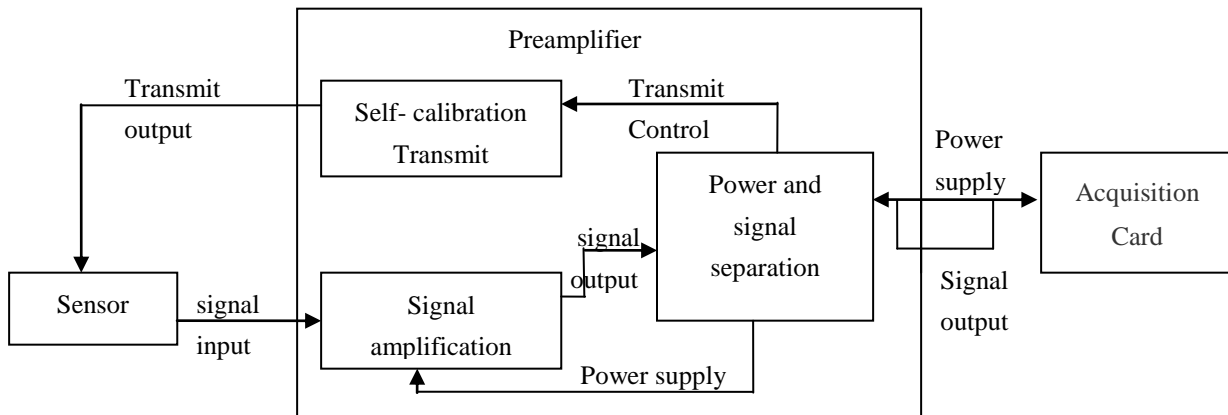


Figure 9. The Principle Structure of the Experiment



Figure 10. the PAI Preamplifier

b.iii SAEU2S Acoustic emission instrument

The SAEU2S acoustic emission instrument (shown in figure 11) is mainly composed of SAEU2 acquisition card, power supply and chassis shell. The principle of the acquisition card is shown in Figure 12



Figure 11. SAEU2S Acoustic Emission Instrument

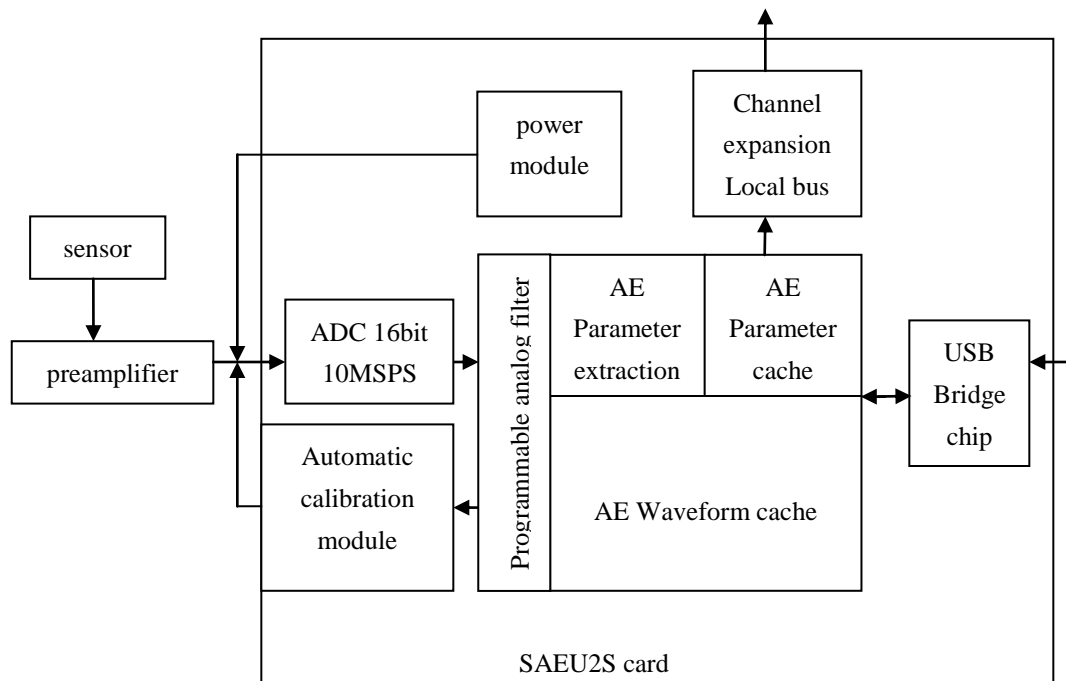


Figure 12. The Principle of the Acquisition Card

The communication between the SAEU2S acoustic emission card and computer is through USB2.0 interface. Each Collection card can get the real characteristic parameters of AE signal. It also can set the trigger threshold of the Waveform and parameters. The data throughput of the real-time continuous acoustic emission characteristic parameters is more than 400 thousand sets per second. The throughput of real-time continuous wave data is greater than 30MB/ seconds. The Maximum single wave sampling is 128K per channel at the same time .Each card has 2 independent channels. The channel number can be extended to 200 .Each card has 4 external parameters of channel which can support 12 input channel parameters. The system built-in AST function that can emit acoustic emission signals.

### c. Experimental Results & Analysis

It does acoustic emission detection experiment on carbon /epoxy three-dimensional braided composites. The experiment locates the defect of every single pore and every micro crack in plate specimen and measures each defect for five times. Then it does cutting & polishing on locating areas and adopts high-resolution CCD microscopic camera to analyze the mesoscopic morphology of defects (micrography method) [ 9 -10] and provides the preliminary experimental basis for the establishment of defect recognition on acoustic emission non-destructive testing in carbon/epoxy three-dimensional braided composites. This paper mainly focuses on three specimens including normal specimen, specimen with micro crack defect and specimen with pore defect for explanations. The characteristics of acoustic emission signals of different types of specimens are also different.

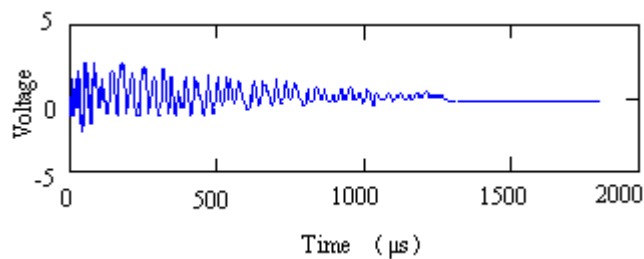


Figure 13. Chart for Acoustic Emission Waveform of Normal Specimen 1

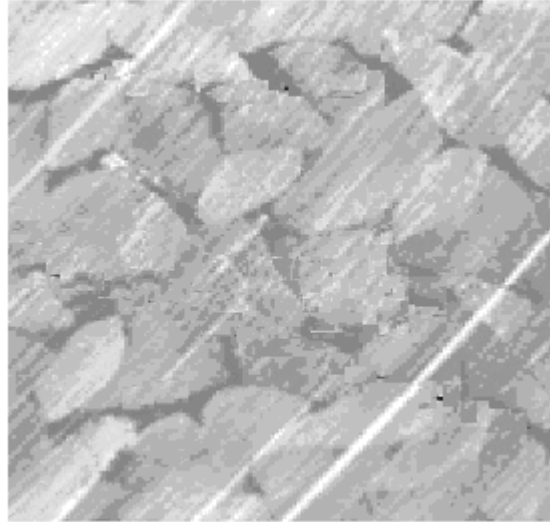


Figure 14. Cross-section Drawing of Normal Specimen 1

Specimen 1 is a normal specimen. The waveform of its acoustic emission signal is smooth and clear. Its amplitude change is also stable, with natural attenuation and no mutation. It is just as shown in Figure 13.

The mesoscopic morphology of the corresponding anatomical plane of the waveform of specimen 1 is just as shown in Figure 14 (In it, the bright stripe that is regularly and obliquely distributed with black and white color is just the grinding crack of metallographic sandpaper on specimen when doing polishing operation). In composite materials with cutting direction, the resin area among fiber bundles is uniformly distributed. This shows that the interlocking weaving structure of fiber bundles is uniform, the interface bonding between fiber bundles and resin is better and no defects like pores and cracks are found.

In the acoustic emission waveform of specimen 2 with the defect of micro cracks, there occurs the phenomenon of obvious amplitude decrease, which shows that it is caused by medium discontinuity in the process of propagation of sound waves. It is just as shown in figure15.

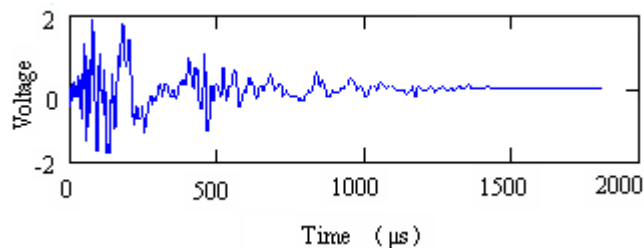


Figure15. Chart for Acoustic Emission Waveform of Specimen 2 with Defect of Micro Cracks

Figure 16 exhibits the mesoscopic cross-section image of specimens with cracks. Among fiber bundles that are interweaved in the cutting direction appears resin-rich area and between fiber bundles and resin appear two obvious cracks in a row.

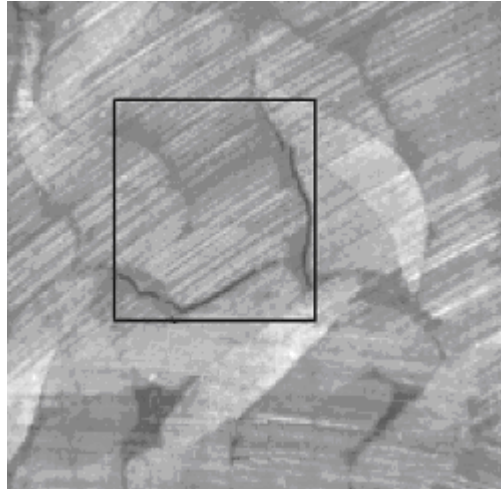


Figure 16. Cross-section Drawing of Specimen 2 with Defect of Micro Cracks

In acoustic emission testing of specimen 3 with internal pore defects, the amplitude of waveform is decreased and the waveform cycle gets smaller, making the waveform become sharper (as shown in Figure 17) . This is mainly due to the phenomenon that the pore surface is smoother than micro crack surface and interior of pores is filled with the air.

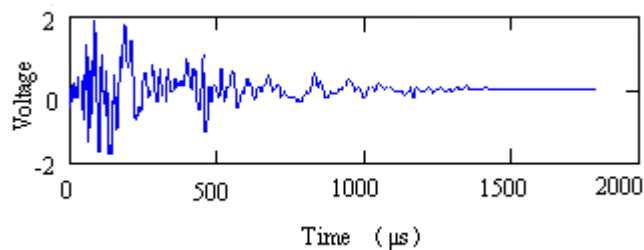


Figure17. Chart for Acoustic Emission Waveform of Specimen 3 with Single Pore

Figure 18 shows the mesoscopic cross-section image of specimens with pores. Among interweaved fiber bundles appears a small piece of resin area and inside this region appears a tiny pore. The pore surface is relatively smooth, with smaller diameter and smaller depth.

Sixteen frequency bands can be obtained by using db6 wavelet to do four-layer decomposition of gathered acoustic emission signals in this experiment. The sampling rate of signals is 2MHz and the width of the

corresponding frequency for each frequency band is 125kHz. Reconstruct the composed signals in the fourth layer, extract the energy of signals on all frequency bands and do the normalization processing on eigenvectors which are composed by them as the input of wavelet neural network.

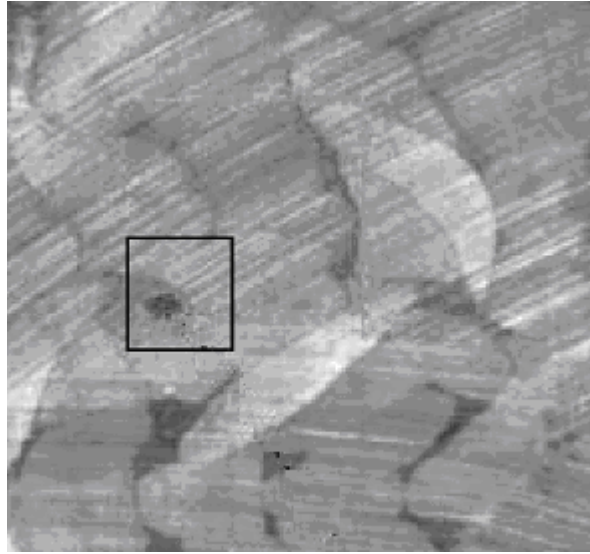


Figure 18. Cross-section Drawing of Specimen 3 with Single Pore

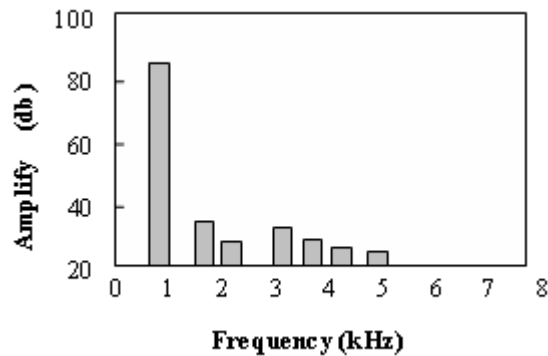


Figure 19. Energy Diagram of Micro Crack Wavelet Packet

The wavelet coefficient of signals after wavelet decomposition describes the basic characteristics of original signals and reflects the characteristic information of material defect signals. Figure 19 and Figure 20 are energy distribution diagrams of all frequency bands after the wavelet packet decomposition of internal defects.

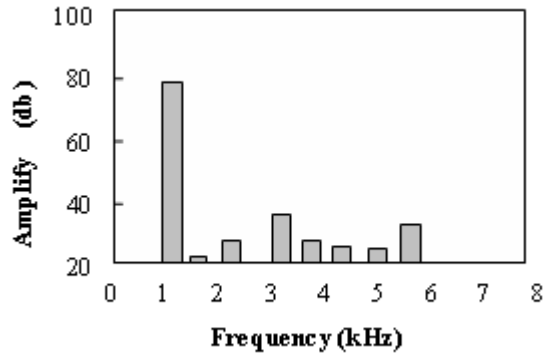


Figure 20. Energy Diagram of Single Pore Wavelet Packet

From figure 18 to figure 99, it can be known that the frequency distribution and amplitude of main energies of different types of acoustic emission signals are different. And the energy of micro crack signals is principally distributed in the frequency range of 50~110kHz and the energy of pore signals is mainly distributed in the frequency range of 120-150 kHz. The energy distribution frequency ranges of these two defects overlap with each other, but the energy amplitude of micro crack signals is slightly higher than that of pore signals.

Do a large number of acoustic emission detections on carbon/epoxy three-dimensional braided composites, gather 8 cracks and 6 pores, do detection on each defect for 5 times after defect location and totally get the feature space of 70 samples(40 micro cracks and 30 pores). Then send the samples to the computer for three-layer wavelet packet decomposition, extract eight energy eigenvalues for each sample and obtain  $70 \times 8 = 560$  neural network inputs after the normalization. The some input data are shown in Table2. In testing process, select the normalized eigenvalues of 35 samples among it (20 crack samples and 15 pores) as the training samples to input the established neural network module for training and use the other eigenvalues as detection samples. Figure 21 shows the network training process. It can be seen that after training, the error reaches 0.006 and it can meet the requirement of system application.

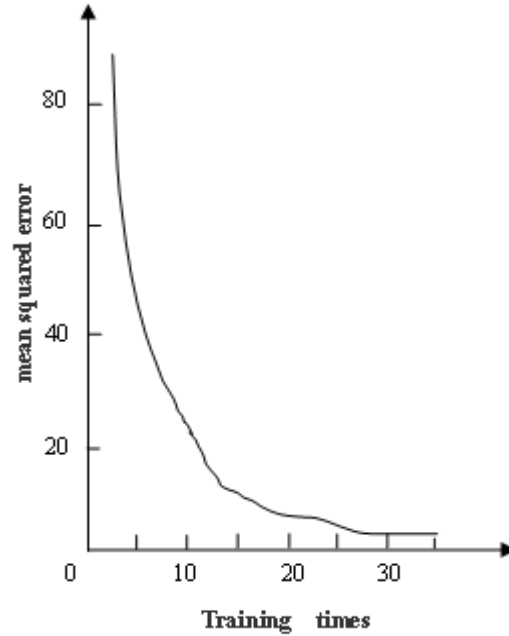


Figure 21. Network Training Error Curve

Table2: input energy eigenvalue of neural network

Sample NO.	Nodes NO.							
	0	1	2	3	4	5	6	7
Crack samples 1	0.2267	0.3101	0.5799	0.3351	0.2801	0.2997	0.2370	0.4299
2	0.2390	0.3707	0.5889	0.2954	0.2864	0.3373	0.2131	0.3607
3	0.2198	0.3978	0.5104	0.3071	0.2701	0.3312	0.2104	0.3899
⋮	⋮	⋮	⋮	⋮	⋮	⋮	⋮	⋮
40	0.2604	0.2591	0.5401	0.2424	0.3106	0.3029	0.2389	0.3724
Pore samples 41	0.4695	0.1049	0.2068	0.1961	0.3169	0.1211	0.5163	0.5226
42	0.4734	0.1125	0.2354	0.2011	0.3185	0.1333	0.4938	0.6017
43	0.4311	0.1051	0.3063	0.2671	0.2921	0.2143	0.4917	0.5921
⋮	⋮	⋮	⋮	⋮	⋮	⋮	⋮	⋮
70	0.4621	0.1544	0.3102	0.1899	0.2877	0.1956	0.5851	0.5766

The trained BP neural network is used to do testing on other 35 samples (20 crack samples and 15 pore samples). The experimental results are as shown in table3.

Table 3: System defect recognition results

<b>Defect Types</b>	<b>Number of Samples</b>	<b>Number of Correct Recognition</b>	<b>Undetected Number</b>	<b>Recognition Rate/%</b>
Micro Cracks	20	16	4	80
Single Pore	15	13	2	86.07
Totalled	35	29	6	82.8

## V. CONCLUSION

(1) Compared with normal specimens, the energies of acoustic emission signals of specimens with single defect are highly different from each other in specific frequency range. And the defect position can trigger energy increase of acoustic emission signals of materials in a certain corresponding range.

(2) The undetected rate of micro crack defect in three-dimensional braided composites reaches 20%, which is mainly caused by the relative complicity of micro cracks and the shape of them in composites and the randomness of crack length & depth.

## REFERENCES

- [1] Wan ZhenKai, "Acoustic Emission Analysis of The Flexural and Tensile properties of 3-D Braided Composite Materials", Journal of Textile Research, Vol 28, No.4, pp-53-55 ,2007.
- [2] Whitwoth HA, " Evaluation of the residual strength degradation in composite laminates under loading", Composite structures, Vol 48,No.4,pp-261- 264,2011.
- [3] Wan Zhenkai, Wang Zhangang, "Reserch on Flaw Detection for Composite Material Using Ultrasonic Testing Based on Neural Network ", Journal of Textile Research, Vol 31,No.2,pp-55-59, 2010 Feb.
- [4] Wenfeng Hao , Yanan Yuan, Xuefeng Yao, Yinji Ma, "Computational analysis of fatigue behavior of 3D 4-directional braided composites based on unit cell approach", Advances in Engineering Software 82 pp-38-52,2015
- [5] Drach A, Drach B, "Tsukrov I.,Processing of fiber architecture data for finite element modeling of 3D woven composites", Advances in Engineering Software ,72:pp-18-27,2014.

- [6] Dong J, Feng M. , “Asymptotic expansion homogenization for simulating progressive damage of 3D braided composites”, *Composite Structure* 92:873 – 82,2010.
- [7] Giovanni Perillo, Frode Grytten, Steinar S, Virgile Delhaye, “Numerical/experimental impact events on filament wound composite pressure vessel”, *Composites: Part B*, vol 69, pp.406 – 417, 2015.
- [8] Mesut Uyaner, Memduh Kara, Aykut S\_ahin, “Fatigue behavior of filament wound E-glass/epoxy composite tubes damaged by low velocity impact”, *Composites: Part B*, vol61,pp. 358 – 364,2014.
- [9] Bilisik K., “Multiaxis 3D Woven Preform and Properties of Multiaxis 3D Woven and 3D Orthogonal Woven Carbon/Epoxy Composites”, *Journal of Reinforced Plastics and Composites*, Vol29,No.8,pp-1173-1186,2010.
- [10] Karahan M, Lomov SV, Bogdanovich AE, “ Fatigue tensile behavior of carbon/epoxy composite reinforced with non-crimp 3D orthogonal woven fabric” ,*Composites Science and Technology*, Vol71,No.16, pp-1961-1972,2011 .
- [11] Wei Fan, Jia-lu Li, Yuan-yuan Zheng, “ Improved thermo-oxidative stability of three-dimensional and four-directional braided carbon fiber/epoxy hierarchical composites using graphene-reinforced gradient interface layer”, *Polymer Testing* 44,pp-177-185,2015.
- [12] Zaman W, Li K, Ikram S, Li W, Zhang D, Guo L. “Morphology, thermal response and anti-ablation performance of 3D-four directional pitch-based carbon/carbon composites”, *Corros Sci* 61:134 – 42,2012.
- [13] Ozaki, H., Omura, Y. “An advanced nonlinear signal model to analyze pulsation-derived photoplethysmogram signals”, *International Journal on Smart Sensing and Intelligent Systems*, Vol.8, No. 2, pp-921-943, 2015.
- [14] Salah H. R. Ali, “Method of optimal measurement strategy for ultra-high-precision machine in roundness nano-metrology” , *International Journal on Smart Sensing and Intelligent Systems*, VOL. 8, NO. 2, pp-896 – 920,June 2015 .
- [15] Adam Funnell, Xiaomin Xu, Jize Yan, Kenichi Soga, “Simulation of noise within BOTDA and COTDR systems to study the impact on dynamic sensing” , *International Journal on Smart Sensing and Intelligent Systems*, VOL. 8, NO. 3,pp-1576 – 1600,Sep. 2015.